Stability of topological solitons in modified two-component Ginzburg-Landau model

Juha Jäykkä*

Department of Physics and Astronomy, University of Turku, FI-20014 Turku, Finland
(Received 2 February 2009; published 6 March 2009)

We study the stability of Hopfions embedded in a certain modification Ginzburg-Landau model of two equally charged condensates. It has been shown by Ward [Phys. Rev. D **66**, 041701(R) (2002)] that a certain modification of the ordinary model results in a system which supports stable topological solitons (Hopfions) for some values of the parameters of the model. We expand the search for stability into a previously uninvestigated region of the parameter space, charting an approximate shape for the stable/unstable boundary and find that, within the accuracy of the numerical methods used, the energy of the stable knot at the boundary is independent of the parameters.

I. INTRODUCTION

Topological solitons, be it vortices, knots, instantons, or other objects, enjoy widespread interest within many fields of physics, perhaps most notably in the fields of particle physics and condensed matter, where these objects invariably occur as solutions of the field equations. In condensed matter physics, topologically stable vortices are also a routinely seen in experiments. Therefore, it is crucial to understand the basic properties of topological solitons in the Ginzburg-Landau and related models. It is against this background that we have studied the static Ginzburg-Landau model, also known as the Abelian Higgs model. Some years ago, it was demonstrated that the archetypal 3D classical field model supporting topologically stable *closed* vortices, the Faddeev-Skyrme (FS) model [1–9], can be embedded in the Ginzburg-Landau model by a change of variables [10]. There was also an earlier work, where the FS model was obtained from the Ginzburg-Landau model in a derivative expansion [11], but this method does not allow for the investigation of solitons in the Ginzburg-Landau model since it does not correspond to any parameter limit. It was further conjectured in Ref. [10] that the two-component Ginzburg-Landau model should, due to this embedding, also support the same topological structures as the FS model does, but more recent studies do not support this conjecture [12,13]. However, Ward found [12] that by modifying the model suitably, stable closed vortices appear as minimum energy configurations of the theory. We expand on Ward's work and find the stable/unstable boundary in the (κ, η) parameter space of the model. We also find that the energy of the stable minimum energy configuration along the said boundary is constant (to within the accuracy of the methods used). The results presented here should also be useful in constructing such initial configurations in the Ginzburg-Landau model which relax into a local, nonzero energy minimum instead of the global one and thus provide a way to construct knotted solitons in the Ginzburg-Landau model.

II. THE MODEL

The static Abelian Higgs model with two charged Higgs bosons is mathematically the same as the Ginzburg-Landau model with two flavors of Cooper pairs or superfluids. The paper will use the following notations. The indices run as follows: $j, k, l \in \{1, 2, 3\}$, $\alpha \in \{1, 2\}$, $\mu, \nu, \iota \in \{0, 1, 2, 3\}$, the fields are $\Psi = (\psi_1 \quad \psi_2)^T$, $F_{\mu\nu} \equiv \partial_\mu A_\nu - \partial_\nu A_\mu$, $\boldsymbol{B} = \epsilon^{jkl}\partial_k A_l$, and the gauge-covariant derivative has the form $D_\mu \equiv \partial_\mu - i\frac{2e}{\hbar c}A_\mu$; when working in three dimensions ($\mu \in \{1, 2, 3\}$) we will also write $\boldsymbol{D} \equiv \nabla - i\frac{2e}{\hbar c}\boldsymbol{A}$. With these notations, the standard Lagrangian density of the two-component Ginzburg-Landau model can be written as

$$\mathcal{L} = \frac{\hbar^2}{2m_\alpha}\|D_\mu \psi_\alpha\|^2 + V(\psi_1, \psi_2) - \frac{1}{4}F_{\mu\nu}F^{\mu\nu}, \quad (1)$$

which gives the static energy density

$$\mathcal{E} = \frac{\hbar^2}{2m_\alpha}\|\boldsymbol{D}\psi_\alpha\|^2 + V(\psi_1, \psi_2) + \frac{1}{2\mu_0}\|\boldsymbol{B}\|^2, \quad (2)$$

where we have used SI units. The form of the potential is not very important as long as it maintains the $SU(2)$ symmetry of Ψ and enforces the condition $\|\Psi\| = $ constant $\neq 0$ at some limit of the parameters of the potential; here we have used

$$V(\psi_1, \psi_2) = \frac{1}{2}\eta(|\Psi|^2 - 1)^2. \quad (3)$$

The electric coupling constant displays an explicit factor of 2 due to the interpretation of the Ginzburg-Landau model as a superconductor, where the ψ_α become Cooper pairs. For computational purposes, it is practical to use natural units, where $\hbar = c = \mu_0 = 1$ and rescale the fields by $\psi_\alpha \to \psi_\alpha \sqrt{m_\alpha}$. For flexibility, we retain a freely selectable electric charge but replace $2e \to g$, finally obtaining the energy density (now $D_k = \partial_k - igA_k$)

*juolja@utu.fi

$$\mathcal{E} = \tfrac{1}{2}\|D\psi_\alpha\|^2 + V(\psi_1, \psi_2) + \tfrac{1}{2}\|B\|^2. \qquad (4)$$

The remainder of this paper will be in natural units.

The embedding of Babaev *et al.* [10] is such that a closed vortex can be defined by the fields ψ_α, leaving the gauge field A free. Using the new variables thus introduced, one can define a vector field n as follows. Let σ be the usual Pauli matrices. We then define

$$n := \begin{pmatrix} \psi_1^* & \psi_2^* \end{pmatrix} \sigma \begin{pmatrix} \psi_1 \\ \psi_2 \end{pmatrix} = \begin{pmatrix} \psi_1^*\psi_2 + \psi_1\psi_2^* \\ i(\psi_1^*\psi_2 - \psi_1\psi_2^*) \\ |\psi_1|^2 - |\psi_2|^2 \end{pmatrix},$$

where we demand that $|\Psi| > 0$ everywhere, consider Ψ normalized to unity, and $\lim_{x\to\infty} n = n_\infty$ exists in order to obtain a map $S^3 \to S^2$. Now the preimage of $-n_\infty$ forms a closed loop, the vortex core.

The fact that A is left free means that there is no non-trivial topology imposed on it and since in the vacuum of the Ginzburg-Landau model A is pure gauge, the magnetic field energy can vanish in all cases. This in turn means that there is no longer a fourth-order derivative in the energy density (4) and Derrick's theorem [14] states that no stable, topologically nontrivial solutions of the field equations with nonzero energy exist. Therefore, the collapse of the magnetic field must be somehow prevented in order to obtain stable topologically nontrivial configurations in the model. There are several physical arguments that suggest there might exist physical processes that prevent the collapse, but here we follow the path set out by Ward, who used a geometrical argument, by adding into the Lagrangian the term [we denote $\Psi^\dagger = (\psi_1^* \ \psi_2^*)$]:

$$\mathcal{L}_W = \tfrac{1}{2}\kappa^2 \|\Psi^\dagger D_\mu \Psi\|^2, \qquad (5)$$

which makes the Ginzburg-Landau -Ward energy density

$$\mathcal{E}_{\mathrm{GLW}}(x) = \overbrace{\tfrac{1}{2}\|D\Psi\|^2}^{\equiv \mathcal{E}_K} + \overbrace{\tfrac{1}{2}\|\nabla \times A\|^2}^{\equiv \mathcal{E}_B} + \overbrace{\tfrac{1}{2}\kappa^2\|\Psi^\dagger D\Psi\|^2}^{\equiv \mathcal{E}_W} + \overbrace{V(\psi_1, \psi_2)}^{\equiv \mathcal{E}_P} \qquad (6)$$

and denoting for any subscript z: $E_z = \int d^3x \mathcal{E}_z$ we finally have the total energy

$$E_{\mathrm{GLW}} = E_K + E_W + E_B + E_P. \qquad (7)$$

The extra term, when the parameters $\kappa, \eta \to \infty$, ensures that the model becomes exactly the Faddeev-Skyrme model

$$\mathcal{E}_{\mathrm{FS}} = \tfrac{1}{2}\|\partial_k n\|^2 + \tfrac{1}{2}g_{\mathrm{FS}}\|n \cdot \partial_j n \times \partial_k n\|^2 \qquad (8)$$

and therefore the model supports, at least asymptotically, stable topologically nontrivial configurations; these solutions are called knot solitons due to their general shape. This limit of $\kappa \to \infty$ was apparently first observed by Hindmarsh [11], albeit in a slightly different context.

Ward studied the question whether the solutions of the limiting model remain stable at finite values of κ, η. It was found that if $\eta = \kappa^2 + 1$, there are knot solitons already at $\kappa = 7.1$. This is due to the fact that the extra term prevents the (total) collapse of the magnetic field, but only when κ, η are large enough: for smaller values, no solutions were found in Ref. [12], although one was found in Ref. [15].

It was recently discovered independently by Babaev [16] by using physical arguments and by Speight [17,18] by giving a rigorous mathematical proof, that the energy of the model has no topological lower bound, even when $\mathcal{L}_W$ is added, but instead for all values of the Hopf invariant, the energy can go to zero. Therefore any stable configurations found are necessarily only local minima of the energy; on the other hand, although the plain Ginzburg-Landau model does not seem to have any stable topologically nontrivial configurations, they may only be very difficult to find due to a very small attraction basin of said configurations, thus requiring very good initial guesses. Investigating such configurations in closely related models may help in finding these initial configurations.

In Ref. [12] Ward investigated only configurations where $g = 1$ and $\eta = \kappa^2 + 1$. We will now present results for the stable/unstable boundary $\eta(\kappa)$ for $g = 1$ and $\kappa \in \{6, 20\}$. It was natural to start the investigation from the values explored by Ward and expand the range of κ in both directions; the limits of this range were eventually set by available computer capacity.

It is also worth noting that, as usual, Derrick's theorem provides a virial theorem for the model. Assume we have a solution of the field equations, Ψ, A and consider its energy density under uniform scaling of the coordinates $x \to \gamma x$:

$$E_{\mathrm{GLW}}(\gamma) = \int d^3x (\mathcal{E}_K(\gamma x) + \mathcal{E}_W(\gamma x) + \mathcal{E}_B(\gamma x) + \mathcal{E}_P(\gamma x)), \qquad (9)$$

which is the starting point of Derrick's theorem. Now, following the method used by Derrick, we get after the change of integration variables $x \to \gamma x$,

$$E_{\mathrm{GLW}}(\gamma) = \gamma E_K + \gamma^{-1}E_B + \gamma E_W + \gamma^3 \qquad (10)$$

differentiating with respect to γ we get

$$\gamma^{-2}E_B = E_K + E_W + 3\gamma^2 E_P. \qquad (11)$$

The stability under scaling requires that this equation holds for $\gamma = 1$, since otherwise some other size would be

energetically more favorable. Thus we have a virial theorem:

$$E_B = E_K + E_W + 3E_P. \qquad (12)$$

This must hold for all stable minimum energy configurations, regardless of the parameter values or value of Hopf invariant (topological charge). For the remainder of the article, the energy is rescaled by

$$E = \frac{E_{\mathrm{GLW}}}{4\pi^2 \sqrt{2}}$$

and we shall always use E for energy. This rescaling is motivated by Ref. [19] and eases comparisons with Ref. [12].

III. NUMERICAL METHODS

We have discretized the system using single-step forward differences on a rectangular cubic lattice. Since the energy of the Ginzburg-Landau model is equal to that of the Abelian Higgs model, the discretization method is the standard (dropping the time-dependent part) used for lattice quantum field theories, as described in Refs. [13,20,21].

The use of a single step in the finite differences approximation instead of some more sophisticated alternative with multiple points is simply a trade-off between speed and accuracy. The discretized equations are very long even with single-step differences. This does not incur significant inaccuracy to the computation for two reasons. First, we are interested mainly in the existence of knotted solitons, which is not affected by the less accurate approximation—the exact values of the parameters where the transition from stable to unstable domain, however, do suffer from inaccuracies as shall be described later. Second, there is no accumulation of error during the iterative process in the optimization algorithms employed.

The term $\mathcal{E}_W$ was discretized in the same manner as the kinetic term: we denote $\boldsymbol{\mu}_j^l = (\delta_j^1, \delta_j^2, \delta_j^3)\nu^l,\ \nu^l \in \{0, 1\}$ and find all gauge invariant discrete terms of the forms

$$\psi_1^*(x + \boldsymbol{\mu}_j^0)\psi_1(x + \boldsymbol{\mu}_j^1) \quad \text{and} \quad \psi_2^*(x + \boldsymbol{\mu}_j^2)\psi_2(x + \boldsymbol{\mu}_j^3),$$

where $\nu^0 + \nu^2 = \nu^1 + \nu^3$, $\sum_l \nu^l < 4$, and

$$\psi_1^*(x + \boldsymbol{\mu}_j^0)\psi_1(x + \boldsymbol{\mu}_j^1) \quad \text{and}$$
$$\psi_2^*(x + \boldsymbol{\mu}_j^2)\psi_2(x + \boldsymbol{\mu}_j^3)e^{\pm iagA_k(x)},$$

where $\sum_{j=0}^3 \nu^l = 1$. There are 18 such terms, which are then multiplied by such constants that the sum of the multiplied terms has the correct continuum limit. This produces the most general single-step forward-differences discretization of $\mathcal{E}_W$.

Energy minimization was done using several different gradient-based optimization methods: steepest descents (SD), Fletcher-Reeves (FR) [22], and Polak-Ribière (PR) [23] versions of the conjugate gradient method and Broyden-Fletcher-Goldfarb-Shanno (BFGS) quasi-Newton method [24–27]. Of these a few simple speed tests were conducted, with the result that the FR method is usually fastest, but sometimes the SD method is faster due to the fact that the other methods spend too much time performing the line searches. (The effect of using less accurate line searches was not investigated.) All the methods are based on gradient directions and thus will only provide a local minimum. Some of the final configurations were subjected to simulated annealing in order to see how deep the minimum is. The annealing could not escape the minimum in a reasonable amount of time, making it reasonable to believe the minima are relatively deep. We did not have the computational resources to perform simulated annealing optimizations of all cases due to the extreme slowness of the algorithm.

As a test of the accuracy and validity of the programs used, we reproduced the results of Ref. [12], Sec. 3. The results agree to within 5%, where our energies are always higher; this confirms the correctness of the program and also gives some indication as to the accuracy compared to other methods. The accuracy of our method could be increased by using larger lattices and smaller lattice constants, but this kind of brute force approach would require excessive amounts of memory—we use more than half a terabyte at maximum—so some more sophisticated methods would be needed.

IV. RESULTS

The search for the boundary between stable and unstable domains of (κ, η) was done as follows. First, an initial state was set up in a cubic 180^3 lattice with a lattice constant of $1/18$. The initial configuration was constructed so that none of the xyz axes coincide with the axial symmetry of the soliton. This configuration was then minimized using one of the above algorithms and various combinations of (κ, η) to determine the rough shape of the boundary. This initial search is done in a small lattice in full knowledge that it may not be large enough to accurately distinguish between configurations which are truly unstable and those that are unstabilized due to the large value of the lattice constant. Indeed, all the unstable systems at the boundary found in this initial search were later proven to be stable in a more accurate lattice. The search consisted of 72 computer runs, but due to the small lattice, used relatively little computer time and gave us the rough values around which to start searching for the boundary in a more accurate lattice. The number of these computationally much more expensive runs was 81.

The values of (κ, η) were then refined in lattices ranging from 360^3 to 600^3. Some unstable configurations were also

put into lattices of sizes up to 720^3 to support the conclusion that the instability is real and not caused by discretization effects. None of these were thus stabilized. The virial theorem equation (12) was then checked for the stable configurations at the boundary (i.e. for each κ the stable configuration with lowest η) to see if the configuration really is a solution. Allowing for a 10% inaccuracy, those that were within the tolerance were considered solutions of the energy minimization. These points are used to sketch the boundary of the stable configurations. Those that were outside the tolerance were further investigated. The reason for inaccuracy proved usually to be due to the small physical dimensions of the computational lattice: the knot suffers from pressure exerted by the edge of the box and cannot reach its preferred size. These configurations were therefore put into a larger lattice with the same lattice constant, minimized and the accuracy was checked again. This process was repeated as many times as necessary to achieve the desired accuracy—except for two cases as we will describe later. Whenever the accuracy was reached, the configuration was considered a solution and added to those used to sketch the boundary. For some cases the accuracy was simply a question of lattice constant; these were recomputed with the same physical dimensions but a smaller lattice constant in order to reach the desired accuracy.

The exceptional cases where the process of putting into a larger box until accuracy is achieved was not completed, where the pairs $(\kappa, \eta) \in \{(10, 0.2), (20, 0.14)\}$. These are stable configurations, but the accuracy goal could not be achieved with the computational capability available due to the cubic growth of memory requirements of increasing the lattice size.

After completing the above process, we select for each κ the stable configurations with lowest η; we denote this value by $\eta_\kappa^{\min}$. The values $(\kappa, \eta_\kappa^{\min})$ are displayed as solid black circles in Fig. 1 together with a curve $\eta(\kappa)$ sketching the approximate shape of the continuous boundary and yellow circles for the largest unstable values of η. Configurations for different values of κ are not always produced in a lattice of the same size, but despite that, the boundary curve fits rather well. All the stable dots in Fig. 1 are confirmed to be solutions by the virial theorem of Eq. (12), except the cases mentioned above: $\kappa \in \{10, 20\}$. The boundary approaches the y axis as $\kappa \to 0$ and x axis as $\kappa \to \infty$. The latter information is not very useful in constructing initial states for normal Ginzburg-Landau model, but the fact that the boundary seems to approach the y axis as well might provide helpful insight and allow the construction of an initial state which could be used to find a topologically stable, nontrivial local energy minimum.

Comparison of the energies of the final configurations reveals that the energy of the solution for (κ, η_κ) is, within our numerical accuracy, independent of κ. This is displayed in Fig. 2, where the dots depict the energies of the
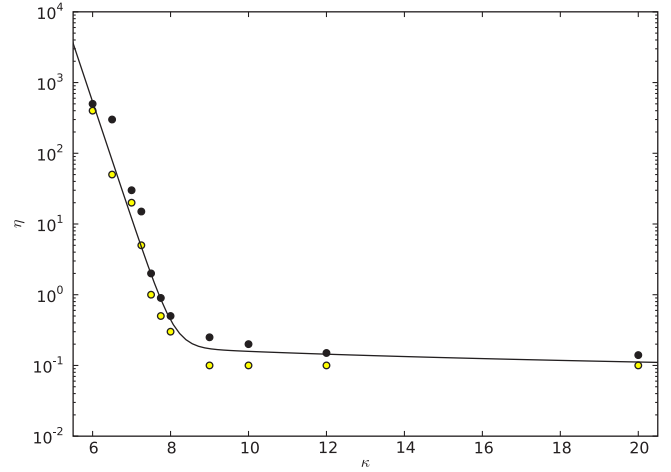

FIG. 1 (color online). Boundary between stable and unstable regions: the solid black circles denote pairs of (κ, η_κ), yellow circles denote the largest unstable values of η, and the curve, $\eta = 45^{7.65-\kappa} + 0.5\kappa^{-(1/2)}$, is a sketch of the boundary.

solutions, the heights of error bars are chosen according to how much the solution deviates from the virial theorem equation (12), and the solid horizontal line is the least-squares fit for the constant energy, neglecting the anomalous cases $\kappa \in \{10, 20\}$. Also, comparing this energy with the energies of the unstable configurations at the moment of loss of topology shows that the unstable configurations always have lower energy than those at the boundary, giving even further support to our argument that the instability is real and not a numerical artefact.

The search for the boundary also provides us, as a byproduct, with information on the shape and size of the final configurations. All solutions have kept their initial orien-
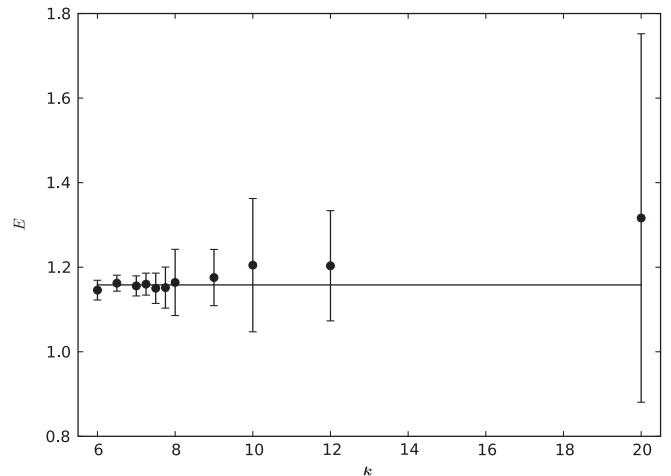

FIG. 2. Energies (black discs) of the stable configurations closest to the boundary, the heights of the error bars show the inaccuracy of the solution as determined from the virial theorem, and the horizontal line is the least-squares fit of a constant energy.
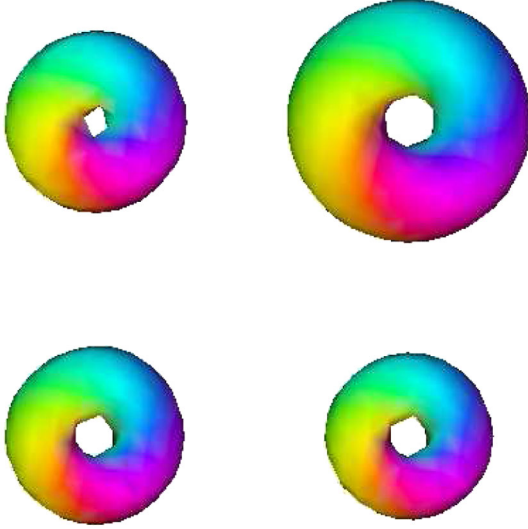
FIG. 3 (color online).   Initial configuration (top left) and three resulting final configurations: $\kappa = 6$ (top right), $\kappa = 8$ (bottom left), and $\kappa = 12$ (bottom right). The colored region is the equator of $\boldsymbol{n}$ (i.e. isosurface where $n_3 = 0$) and the coloring corresponds to the longitude of $\boldsymbol{n}$.

TABLE I.   Terms of the energy function of the final configurations of $\kappa \in \{6, 8, 12\}$.

κ	E_K	E_B	E_W	E_P
6	23.740	32.111	7.6571	0.460 53
8	26.739	31.808	5.9745	0.463 35
12	31.580	32.334	2.5649	0.705 55

tation and overall shape, the only visible difference between the final configurations is the apparent decrease of the size of the torus with growing κ, as shown in Fig. 3 for the cases $\kappa \in \{6, 8, 12\}$. It remains an open question whether the final toroidal configuration obtained from this initial configuration would shrink to zero as $\kappa \to \infty$ because we were unable to follow the boundary above $\kappa = 12$.

Looking at the four terms of the energy function of these final configurations reveals more details of the interplay between the various terms. As can be seen from Table I, E_K increases with increasing κ, but E_W decreases. This is expected since on the limit $\kappa \to \infty$, we must have $E_W \to 0$. Since it was found in [13] that the magnetic field always approaches zero for unstable systems in the nonmodified Ginzburg-Landau model, it is interesting to note that there seems to be no trace of this here: the magnetic energy does not change appreciably. The variation in the potential energy is also negligibly small.

V. CONCLUSIONS

We have studied the existence of local minima in a modified two-component Ginzburg-Landau model and how the energy of these behaves along the boundary where the local minima become unstable. It was found that local minima exist for a wide range of values of the parameter κ, but that there is a limiting value of η for each κ below which the minimum vanishes. It remains open whether there still is a minimum but our initial configuration has simply moved ''closer'' to the global minimum of zero so that the gradient-based algorithms can no longer reach it. Also, there can be other local minima. To explore these possibilities further it is required to use either a set of very different initial configurations or an algorithm which can explore a wide region of the configuration space starting from a single initial configuration such as the genetic algorithm (which has the downside of being able to escape the local minima and thus ending up in the trivial global minimum).

Strikingly, the energy was shown to be constant along the boundary. This information, along with the fact that higher values of η are required for lower values of κ, might provide a way to construct an initial configuration in the ordinary two-component Ginzburg-Landau model, which, under the minimization of energy, would lead to a nonzero local minimum. The procedure would, however, require further insight into how the various terms of the energy functional behave when κ decreases; our numerical scheme was not designed for this and as such, appears not to be accurate enough to provide this information. In contrast to its energy, the size of the minimum energy configuration decreases as κ increases. This requires progressively smaller values of the lattice constant and thus a significantly different numerical approach than the simple, but very large (recall that we used over half a terabyte) lattices used here. Still, the possibility remains of further research in both smaller and larger values of κ, but as they are not addressable by the framework used here, it falls outside the scope of this paper.

[1] L. D. Faddeev, IAS, PRINCETON print-75-0570, 1975.

[2] L. D. Faddeev, in *Relativity, Quanta, and Cosmology*, edited by M. Pantaleo and F. De Finis (Johnson Reprint Corp., New York, 1979), Vol. 1, p. 247.

[3] L. D. Faddeev and A. J. Niemi, Nature (London) **387**, 58 (1997).

[4] R. A. Battye and P. M. Sutcliffe, Phys. Rev. Lett. **81**, 4798 (1998).

[5] R. A. Battye and P. Sutcliffe, Proc. R. Soc. A **455**, 4305 (1999).

[6] J. Hietarinta and P. Salo, Phys. Lett. B **451**, 60 (1999).

[7] J. Hietarinta and P. Salo, Phys. Rev. D **62**, 081701(R) (2000).

[8] J. Hietarinta, J. Jaykka, and P. Salo, Phys. Lett. A **321**, 324 (2004).

[9] C. Adam, J. Sanchez-Guillen, and A. Wereszczynski, Eur. Phys. J. C **47**, 513 (2006).

[10] E. Babaev, L. D. Faddeev, and A. J. Niemi, Phys. Rev. B **65**, 100512 (2002).

[11] M. Hindmarsh, Nucl. Phys. **B392**, 461 (1993).

[12] R. S. Ward, Phys. Rev. D **66**, 041701(R) (2002).

[13] J. Jaykka, J. Hietarinta, and P. Salo, Phys. Rev. B **77**, 094509 (2008).

[14] G. H. Derrick, J. Math. Phys. (N.Y.) **5**, 1252 (1964).

[15] A. J. Niemi, K. Palo, and S. Virtanen, Phys. Rev. D **61**, 085020 (2000).

[16] E. Babaev, arXiv:0809.4468v3.

[17] J. M. Speight, arXiv:0812.1493.

[18] J. M. Speight (private communication).

[19] R. S. Ward, Nonlinearity **12**, 241 (1999).

[20] K. G. Wilson, Phys. Rev. D **10**, 2445 (1974).

[21] P. H. Damgaard and U. M. Heller, Phys. Rev. Lett. **60**, 1246 (1988).

[22] R. Fletcher and C. M. Reeves, Computer Journal **7**, 149 (1964).

[23] E. Polak and G. Ribière, Rev. Françeaise Informat. Recherche Opérationnelle **3**, 35 (1969).

[24] R. Fletcher, Computer Journal **13**, 317 (1970).

[25] D. Goldfarb, Math. Comput. **24**, 23 (1970).

[26] D. F. Shanno, Math. Comput. **24**, 647 (1970).

[27] C. G. Broyden, J. Inst. Math. Appl. **6**, 76 (1970).